J|A|C|S
ARTICLES
Published on Web 06/01/2007

Inhibitor Fingerprinting of Matrix Metalloproteases Using a Combinatorial Peptide Hydroxamate Library

Mahesh Uttamchandani,[†] Jun Wang,[‡] Junqi Li,[‡] Mingyu Hu,[‡] Hongyan Sun,[‡] Kitty Y.-T. Chen,[†] Kai Liu,[†] and Shao Q. Yao*[,†,‡,§]

Contribution from the Department of Biological Sciences, Department of Chemistry, and NUS MedChem Program of the Office of Life Sciences, 3 Science Drive 3, National University of Singapore, Singapore 117543

Received February 6, 2007; E-mail: chmyaosq@nus.edu.sg

Abstract: We report the inhibitor fingerprints of seven matrix metalloproteases, representing all five established families of this important class of enzymes, against a highly diversified small-molecule library. A total of 1400 peptide hydroxamates were individually prepared by systematically permuting both natural and unnatural amino acids across the P_1', P_2', and P_3' positions, thereby generating an inhibitor library with three-pronged structural diversity. High-throughput screenings were efficiently conducted in microtiter plate format, providing a rapid and quantitative determination of inhibitor potency across the panel of enzymes. Despite similarities in substrate preferences and structural homologies within this class of enzymes, our findings revealed distinct patterns of inhibition for each MMP against varied chemical scaffolds. The resulting inhibitor fingerprints readily facilitated the identification of inhibitors with good potency as well as desirable selectivity, potentially minimizing adverse effects when developing such leads into candidate drugs. The strategy also offers a novel method for the functional classification of matrix metalloproteases, on the basis of the characteristic profiles obtained using the diverse set of inhibitors. This approach thus paves the way forward in lead identification by providing a rapid and quantitative method for selectivity screening at the outset of the drug discovery process.

Introduction

Matrix metalloproteases (MMPs) are a family of zinc-dependent proteinases that play complex and diverse roles in vivo. Their collective involvement in tissue remodeling is vital for normal physiological development, and stringent control is placed over their activity at both transcriptional and post-transcriptional levels.[1] Minor perturbations of these enzymes consequently manifest in the deregulated catalytic degradation of the extracellular matrix—a defining feature in the pathophysiology of diseases such as cancer, cardiovascular diseases, and arthritis.[2,3] There have accordingly been intense interests in developing effective small-molecule drugs against this class of enzymes.[4] Recent studies have further identified MMPs (namely, MMPs -1, -2, and -7) that directly accelerate tumorigenesis, implicating these enzymes as vital disease targets.[5] In contrast, other closely related members in the MMP family often confer valuable and protective effects in various human diseases. Stromal cells, for example, direct MMP activity beneficially toward tissue homeostasis, enhancing host resistance toward cancer and other abnormalities.[5] Knocking-out certain MMPs (for example, MMPs -3, -8, and -9) has also been directly linked to tumor proliferation in animal models of several cancers, underscoring the positive roles mediated by selective members of the MMP family.[6]

MMPs share conserved mechanisms and flexible active sites. This presents a delicate challenge for the development of compounds that target only aberrant MMPs for therapeutic intervention and exert minimal cross-reactivity or side effects.[7] Several MMP inhibitors that were initially selected and optimized on the basis of good potency came into extensive phase III clinical trials, only to be discovered ineffective because of problems arising from a lack of selectivity.[8,9] This raises a major impetus to rapidly establish better small-molecule inhibitors that not only exhibit good potency but also high selectivity. Ideally, such leads should inhibit only target MMPs (MMPs -1, -2, and -7) responsible for the relevant disease, while minimally affecting any antitarget MMPs (MMPs -3, -8, and -9). MMPs have classically been divided into five families on the basis of their sequence homology, substrate preference, and cellular localization (Supporting Information Table S1). Such a classification, however, provides limited functional information,

[†] Department of Biological Sciences.
[‡] Department of Chemistry.
[§] NUS MedChem Program of the Office of Life Sciences.

(1) Nagase, H.; Woessner, J. F. *J. Biol. Chem.* **1999**, *274*, 21491−21494.
(2) Murphy, G.; Knauper, V.; Atkinson, S.; Butler, G.; English, W.; Hutton, M.; Stracke, J.; Clark, I. *Arthritis Res.* **2002**, *4*, S39−S49.
(3) Mandal, M.; Mandal, A.; Das, S.; Chakraborti, T.; Chakraborti, S. *Mol. Cell. Biochem.* **2003**, *252*, 305−329.
(4) Gourley, M.; Williamson, J. S. *Curr. Pharm. Des.* **2000**, *6*, 417−439.
(5) Overall, C. M.; Kleifeld, O. *Nat. Rev. Cancer* **2006**, *6*, 227−239.
(6) Overall, C. M.; Kleifeld, O. *Br. J. Cancer* **2006**, *94*, 941−946.
(7) Cuniasse, P.; Devel, L.; Makaritis, A.; Beau, F.; Georgiadis, D.; Matziari, M.; Yiotakis, A.; Dive, V. *Biochimie* **2005**, *87*, 393−402.
(8) Overall, C. M.; Lopez-Otin, C. *Nat. Rev. Cancer* **2002**, *2*, 657−672.
(9) Coussens, L. M.; Fingleton, B.; Matrisian, L. M. *Science* **2002**, *295*, 2387−2392.

10.1021/ja070870h CCC: $37.00

especially toward aiding the design or prediction of potent and selective inhibitors for MMPs. In order to address both these pressing challenges, we present a strategy that facilitates the rapid elucidation of inhibitor selectivity and potency through clustered enzyme "fingerprints" generated from high-throughput screening of focused inhibitor libraries.

The general strategy for MMP inhibitor design has involved grafting short peptide chains to zinc binding groups (ZBG).[10] For our study we have adopted the hydroxamate ($CONH-O^-$) group that chelates strongly to the metal center at the enzyme active site and has been exploited in a variety of potent competitive inhibitors against this class of enzymes. In this work, we have overcome the inherent limitations from traditional mixture-based positional-scanning (PS) combinatorial libraries and have created a diverse repertoire of 1400 individual inhibitor scaffolds by adopting the split-pool directed sorting synthesis method.[11] This set of compounds were combinatorially permuted across the P_1', P_2', and P_3' positions, providing expansive chemical diversity to target the active sites of MMPs (and potentially other classes of metalloproteins). Assaying different enzymes against this library rapidly establishes contributions from each of these defined positions toward the overall potency and selectivity of the inhibitors. We herein report the data set acquired by screening a comprehensive panel of seven different MMPs with representation from all five MMP families. The results were further assessed for global activities, specificity, and potency as well as hierarchical clustering, providing unique insights into inhibitor design and preference within this important group of enzymes.

Materials and Methods

Materials. All chemicals were purchased at the highest available grade from commercial vendors and used without further purifications, unless otherwise noted. All reactions were carried out under a N_2 atmosphere with HPLC grade solvents, unless otherwise stated. ESI mass spectra were acquired in both the positive and negative mode using a Finnigan/Mat TSQ7000 spectrometer. Analytical RP-HPLC separations were performed on Phenomex C_{18} column (150 mm × 3.0 mm), using a Shimadzu Prominence HPLC system equipped with a Shimadzu SPD-20A detector. Eluents A (0.1% TFA/acetonitrile) and B (0.1% TFA/water) were used as the mobile phases. Active enzymes were acquired commercially, specifically MMPs -3, -7, -9, and -14 from Calbiochem (Merck, Germany) and MMPs -2, -8, and -13 from Biomol International (Philadelphia, PA). Fluorogenic substrates were purchased from Calbiochem (Merck, Germany) and AnaSpec (California). A commercial broad-spectrum MMP inhibitor, GM6001, was obtained from Calbiochem, (Merck, Germany).

Library Synthesis. Preparation of the hydroxamate inhibitors using solid-phase synthesis was carried out as previously described.[11] Briefly, the construction of the 1400-member library was performed on rink amide resin by standard Fmoc solid-phase peptide synthesis in microreactors (encoded with radiofrequency tags) using the IRORI split-and-pool directed sorting technology.[12,13] The synthesis involved the use of minimal reaction bottles in three rounds of synthesis and sorting. The final products were released from support by standard TFA cleavage and purified by precipitation (Supporting Information Figure S2).[14,15] A biotin linker was incorporated for alternative future applications of the library. The average concentration of individual inhibitors was estimated using aminomethyl carboxycoumarin ($\lambda_{ex/em}$ = 355/460 nm) conjugated as a 1% additive in the final coupling step, as previously described.[11] The final products were dissolved in dimethyl sulfoxide to equivalent concentrations, diluted appropriately, and used directly for subsequent high-throughput biochemical screens. Randomly selected products were positively confirmed by LCMS and shown to be of sufficient purity.

Biochemical Assays. Each enzyme was assayed using a suitable fluorogenic peptide substrate under optimized conditions. The assays were performed in black flat-bottom polypropylene 384-well plates (Nunc, U.S.A.), using 50 μL total reaction volumes. Automated assembly of the reaction components was performed through an eight-channel robotic dispensing system (Precision XS, Biotek, VT). Upon enzyme addition in the final step to initiate the reaction, the plates were incubated at 37 °C for intervals between 1 and 2 h, before being queried for end point fluorescence on a SpectraMax Gemini XS fluorescence plate reader (Molecular Devices, U.S.A.). In total, three different substrates were employed. First, TNO211 (DABCYL-GABA-Pro-Gln-Gly-|-Leu-Glu (EDANS)-Ala-Lys-NH_2; $\lambda_{ex/em}$ = 340/485 nm) was prepared to final screening concentrations of 3 μM for MMP-3 (60 fmol), 6.8 μM for MMP-9 (25 fmol), and 3.4 μM for MMP-14 (200 fmol). The samples were buffered in 100 mM Tris, pH 7.5, supplemented with 300 mM NaCl, 10 mM $CaCl_2$, 2 μM $ZnCl_2$, and 0.02% Brij.[16] Second, MCA-Pro-Leu-Gly-|-Leu-Dpa-Ala-Arg-NH_2 ($\lambda_{ex/em}$ = 325/393 nm) was applied at 3.2 μM and 1.6 μM for screening of MMP-2 (50 fmol) and MMP-7 (600 fmol), respectively.[17] The final substrate, MCA-Pro-Cha-Gly-|-Nva-His-Ala-Dap(Dnp)-NH_2 ($\lambda_{ex/em}$ = 325/393 nm) was optimized for MMP-13 (10 fmol) and MMP-8 (50 fmol) at reaction concentrations of 3.4 and 4 μM, respectively.[18] The latter four enzymes were buffered with 100 mM Tris pH 7.5 supplemented with 100 mM NaCl, 10 mM $CaCl_2$, and 0.05% Brij-35. The optimized amount of enzyme utilized for each assay is italicized in parenthesis next to each named enzyme. The -|- position within the substrate sequence indicates the cleavage site. Each MMP was assayed against the entire 1400-member library (normalized to a final reaction concentration of approximately 660 nM) in staggered runs.

Data Analysis. Plate readings were exported from the scanner SoftmaxPro software into Microsoft Excel. Raw results were normalized by subtracting readings from the initial uncleaved substrate and inhibitor backgrounds. Data points from each plate were benchmarked against positive controls (these were essentially uninhibited samples, with enzymes assayed without inhibitor, replicated at five wells per plate). The relative potencies of each inhibitor were calculated from the normalized data through the following relationship:

$$\text{inhibition potency of } x = \left(1 - \frac{\text{measured intensity, } x}{\text{uninhibited intensity}}\right) \times 100\%$$

The combined data set was also subjected to cluster analysis to correlate specificity information from the library into hierarchical contributions, providing unique inhibition-dependent profiles of MMPs. Averaged linkage clustering was performed using the Systat v11.0 software (San Jose, CA). For comparison, active site domains comprising ~170 amino acid residues of human MMPs were retrieved from MEROPS[19] and clustered using ClustalW.[20] The data set was presented

(10) Rao, B. G. *Curr. Pharm. Des.* **2005**, *3*, 295−322.
(11) Wang, J.; Uttamchandani, M.; Sun, L. P.; Yao, S. Q. *Chem. Commun.* **2006**, 716−719.
(12) Xiao, X. Y.; Li, R.; Zhuang, H.; Ewing, B.; Karunaratne, K.; Lillig, J.; Brown, R.; Nicolaou, C. *Biotechnol. Bioeng.* **2000**, *71*, 44−50.
(13) *Combinatorial Chemistry—A Practical Approach*; Fenniri, H., Ed.; Oxford University Press: New York, 2000; p 432.
(14) Wang, J.; Uttamchandani, M.; Li, J.; Hu, M.; Yao, S. Q. *Chem. Commun.* **2006**, 3783−3785.
(15) Wang, J.; Uttamchandani, M.; Li, J.; Hu, M.; Yao, S. Q. *Org. Lett.* **2006**, *8*, 3821−3824.
(16) Beekman, B.; van El, B.; Drijfhout, J. W.; Ronday, H. K.; TeKoppele, J. M. *FEBS Lett.* **1997**, *418*, 305−309.
(17) Knight, C. G.; Willenbrock, F.; Murphy, G. *FEBS Lett.* **1992**, *296*, 263−266.
(18) Knauper, V.; Lopez-Otin, C.; Smith, B.; Knight, G.; Murphy, G. *J. Biol. Chem.* **1996**, *271*, 1544−1550.
(19) Rawlings, N. D.; Morton, F. R.; Barrett, A. J. *Nucleic Acids Res.* **2006**, *34* (database issue), D270−D272.

Scheme 1. Design of Combinatorial Peptide Hydroxamate Inhibitor Library[a,b]

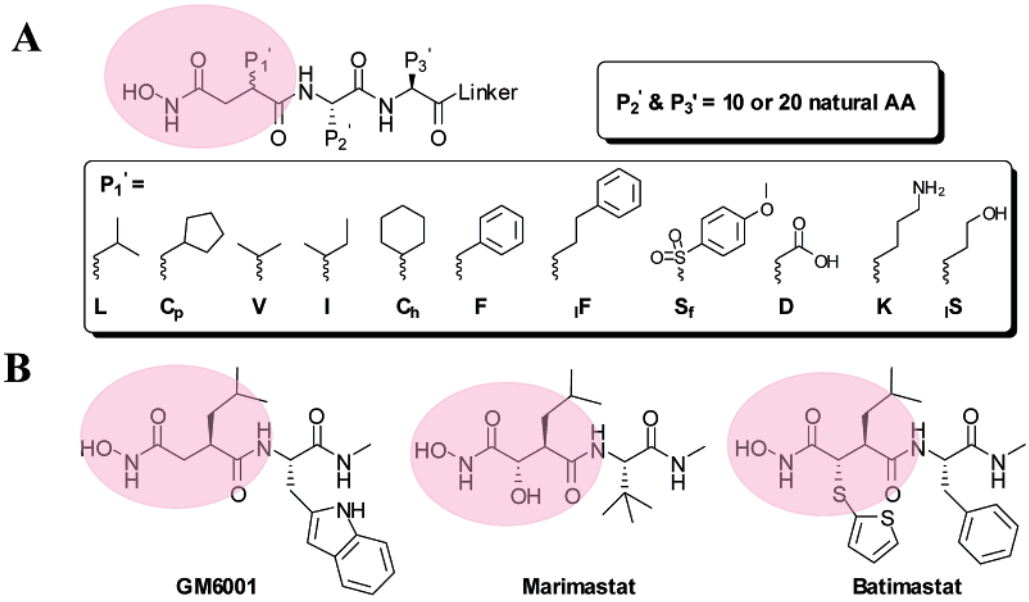

[a] Library was constructed on rink amide resin using split-and-pool directed sorting technology. The P_1' consists of 11 unnatural amino acids made of substituted succinyl hydroxamate ZBG (highlighted in pink). Each was assigned a unique single-letter code (inset). The chemical synthesis of these ZBGs was reported previously (refs 11, 14, and 15). [b]Structures of GM6001, marimastat, and batimastat.

in both 3-D cube plots, performed using the Graphis software (Kylebank, U.K.), and colored heat maps using treeview (http://rana.lbl.gov/EisenSoftware.htm) software. Venn diagrams were generated using the Venn diagram generator (http://www.pangloss.com/seidel/Protocols/venn.cgi).

IC_{50} Measurements. Concentration-dependent measurements were performed to confirm the potency of representative inhibitors within the library set. Inhibitors exhibiting a range of potencies for each MMP were selected from the microplate screens and evaluated using IC_{50} measurements. Briefly, dose-dependent reactions were performed by varying the concentrations of the inhibitor, under the same enzyme concentration. A 2-fold dilution series from approximately 2 μM to 15 nM (final reaction concentration) was prepared for each inhibitor in black 384-well plates. GM6001, a broad-spectrum MMP inhibitor, was also evaluated in a 3-fold dilution series from 4 μM to 5.4 nM (final reaction concentration). Substrates and enzymes were applied according to the conditions earlier optimized. The plates were allowed to incubate for 1−2 h at 37 °C before being interrogated for end point fluorescence. The IC_{50} was calculated by curve fitting against the concentration-dependent fluorescent plots using the Graphpad Prism software v.4.03 (GraphPad, San Diego, CA).

In Silico Docking Experiments. Docking was performed on a SGI IRIX 6.5 workstation using the SYBYL suite (version 7.2) installed with the FlexX docking software. Protein coordinates were obtained from the Protein Data Bank; specifically inhibitor complexed crystal structures with the following accessions were employed: MMP-2: 1QIB, MMP-7: 1MMQ. Structures of representative inhibitors were drawn using the "Sketch Molecule" option, and hydrogens were added. The biotin linker of selected inhibitors was excluded to simplify the docking simulations. The structures were minimized using 100 iterations at 0.05 kcal/mol Å to relieve any torsional strain, and formal charges were assigned. The original protein structures were modified through the removal of water molecules. The docking sphere was set at 10 Å, centered at the zinc residue in the enzyme active site. Applying these criteria, the docking was performed for 30 iterations, with the most optimized configurations displayed. Proteins were displayed as either MOLCAD Connolly surfaces or ribbon diagrams.

(20) Chenna, R.; Sugawara, H.; Koike, T.; Lopez, R.; Gibson, T. J.; Higgins, D. G.; Thompson, J. D. *Nucleic Acids Res.* **2003**, *31*, 3497−3500.

Results

Library Synthesis. Tagging every microreactor enabled the rapid, tractable synthesis of each library member. The chemical synthesis of the 11 succinyl hydroxamates (Scheme 1), representing the different P_1' substituents in the 1400-member peptide library, was previously reported.[11,14,15] The library was prepared in two installments. First, a 400-member sublibrary containing a leucine side chain at the P_1' position (represented with single-letter code **L**) was constructed with permutations of all 20 natural amino acids across the P_2' and P_3' positions. An additional 1000-member set was constructed with 10 different P_1' warheads containing side chains of both natural and unnatural amino acids (Scheme 1). The P_2' and P_3' positions in this set were systematically permuted with 10 representative proteinogenic amino acids, specifically nonpolar (Ala, Leu, Phe, Trp), charged polar (Glu, Lys, His), and uncharged polar (Gln, Ser, Tyr) amino acids. The library design forged a novel and comprehensive set of compounds to target metalloproteases, featuring both a broad structural coverage for the varying depths and sizes of enzyme binding pockets, as well as targeted inhibition through a potent ZBG to direct these molecules into the active sites. The quality of the final products synthesized was confirmed by LCMS of representative samples, indicating most inhibitors (>90%) were of correct molecular mass and sufficient purity (>80%).

Inhibitor Fingerprints of MMPs across P_1'. The profiles of seven MMPs representing all five families of this class of enzymes were determined by high-throughput screening against the 1400 peptide hydroxamates. The results are displayed in individual cube plots for each MMP, with the representations made to potencies by the size and color intensity of individual spheres (positioned spatially across three axes according to their P_1', P_2', and P_3' identities) (Supporting Information Figure S1). The combined data set is further presented as a colored heat map, revealing the unique and discriminating signatures of each small molecule (Figure 1). The assay was independently

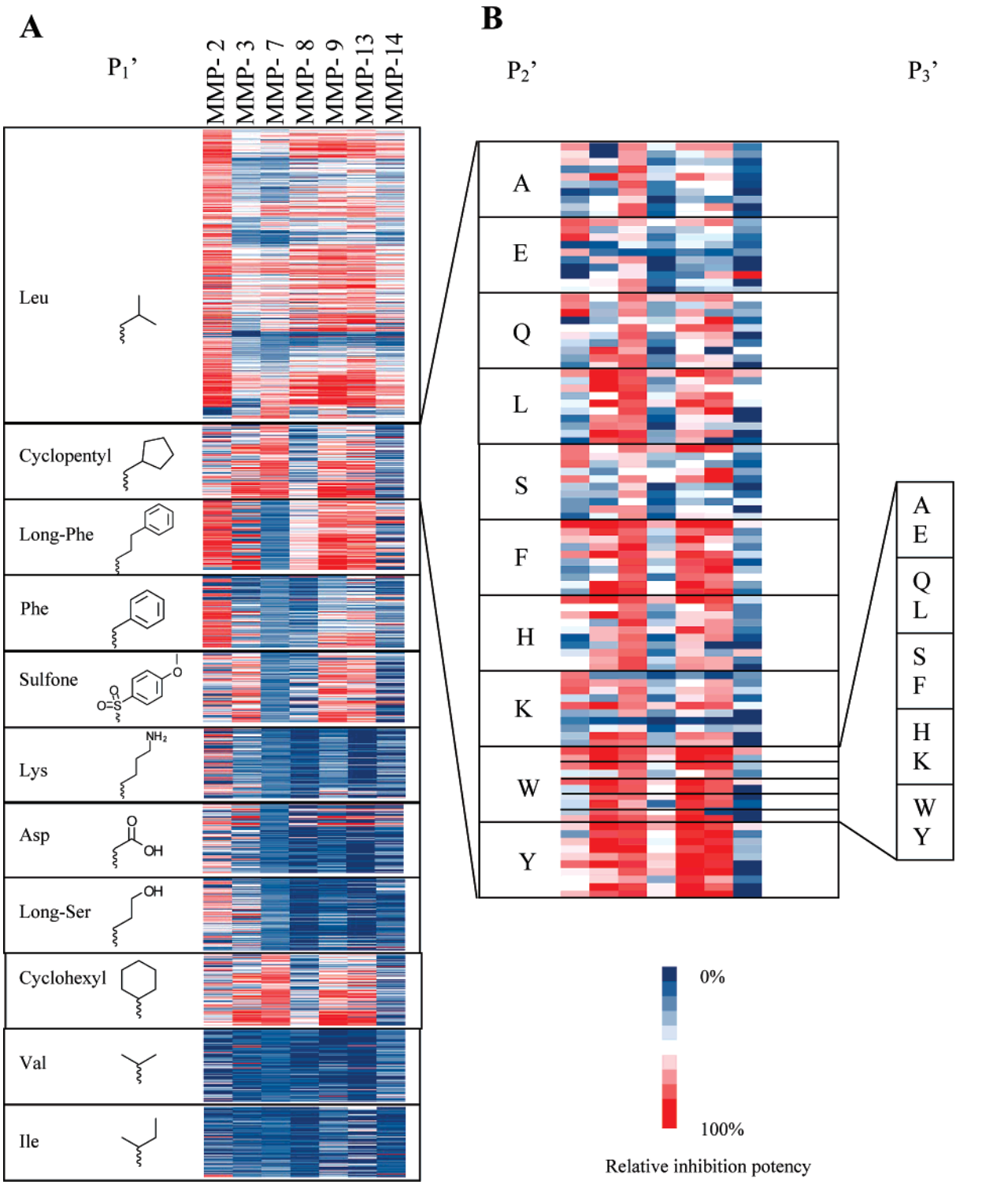

Figure 1. (A) Heat map of 1400 inhibitors profiled against a panel of seven MMPs. The most potent inhibitors are displayed in red, while the least potent inhibitors are shown in blue. (B) Magnified heat map of inhibitors presenting $\mathbf{C_p}$ in the P_1' position against the panel of seven MMPs. The color scale for relative inhibition potency is shown (inset). The P_2' and P_3' substituents are represented by standard single-letter amino acid codes.

reproduced for 100 inhibitors in duplicate to confirm that most (nearly 80%) of the inhibitors gave potencies that were consistent to the large-scale screens (<20% variation in potencies).

All proteases tested were found to be globally inhibited by scaffolds containing a leucine side chain (**L**) at the P_1' position. This is consistent with the general scaffolds of established hydroxamate-based inhibitors such as GM6001, batimastat, and marimastat that serve as potent and broad-spectrum MMP inhibitors (Scheme 1).[10] The cyclopentyl side chain ($\mathbf{C_p}$), which is a cyclic mimic of **L**, also showed strong potencies with a range of MMPs, as did warheads containing aromatic side chains (Phe and long-Phe represented by **F** and $_l$**F**). Inhibitors containing the sulfone side chain ($\mathbf{S_f}$) at the P_1' position were potent against MMPs -2, -3, -9, and -13, probably as a result of favorable H-bond interactions. Cyclohexyl side chain ($\mathbf{C_h}$)

displayed mixed and stronger inhibition potencies against several MMP clusters in comparison with other β-branched P_1' side chains (namely, Val and Ile, represented by **V** and **I**, respectively). The latter appeared the least potent, with none of the MMPs tested showing significant potency with either of these sublibraries. The polar side chains (e.g., Asp, Lys, and long-Ser represented by **D**, **K**, and **$_l$S**, respectively) at the P_1' position also yielded relatively weak inhibitors.

MMPs -8 and -14 were predominantly inhibited by only the **$_l$F** and **L** side chains. Apart from these MMPs, the **$_l$F** side chain was potent against the other deep S_1' pocket enzymes as well, such as MMPs -2, -3, -9, and -13. Interestingly, its natural counterpart, **F**, exhibited a similar pattern of inhibition against the same enzymes, albeit at a lower potency. On the other hand, enzymes with a short S_1' pocket, such as MMP-7, were not inhibited by the larger P_1' warheads, irrespective of the substitutions made to the P_2' and P_3' positions. MMP-7 was nevertheless sensitive to two unique hydrophobic P_1' side chains, namely, $\mathbf{C_p}$ and $\mathbf{C_h}$, confirming recent findings.[14] The $\mathbf{C_h}$ side chain also exhibited potency against MMP-3, while the $\mathbf{C_p}$ moiety was potent against MMPs -2, -3, -9, and -13.

Certain inhibitor sublibraries with narrower selectivity spectrums were also uncovered from the high-throughput screening results. For example, the P_1' side chains containing **D** and **$_l$S** were found to perturb MMPs -2 and -3, at the exclusion of all the other MMPs screened. **K** positioned at the P_1' site provided inhibitors that appeared to only inhibit MMP-2 under the screening conditions employed.

Inhibitor Fingerprints of MMPs across P_2' and P_3'. It was observed that variations across P_2' and P_3' positions contributed more subtly to inhibition. This is consistent with both these subsites presenting solvent-exposed clefts for interaction.[21] These positions were nevertheless important in contributing to overall selectivity and potency. Even within the broadly potent **L** and $\mathbf{C_p}$ sublibraries (Figure 1), substitutions in the P_2' and P_3' positions had a marked effect on selectivity. In the expanded heat map of the sublibrary containing the $\mathbf{C_p}$ side chain at the P_1' position, these contributions are more clearly visualized (Figure 1B). On average, inhibitors presenting aromatic side chains (**F**, **W**, and **Y**) in the P_2' position displayed improved inhibition potencies, as did residues with **S** or **A** at the P_3' positions (Figure 2). This is consistent with various reports describing favorable contributions of similar positions and residues to overall inhibitor potencies.[21,22]

Averaged Inhibitor Fingerprints. In order to better visualize contributions across the different positions, potencies from each of the P_1', P_2', and P_3' side chains in the inhibitor library were averaged and graphically presented (Figure 2). The error bars reflect the standard deviation of the results, to serve as an indication of variance within each combined set. Evidently, the greatest margins of difference in potency came from substitutions at the P_1' site, reinforcing this position's importance to potency. Besides previously mentioned residues that marginally contribute to overall potency, there otherwise appeared to be insignificant potency changes from the P_2' and P_3' positions across all the MMPs. Interestingly, this was somewhat different from the findings where a single amino acid was varied to the scaffold at the same positions; closer examination of individual inhibitor fingerprints clearly indicates measurable effects on inhibition potency as well as selectivity across MMPs (Figure 1B). This analysis thus highlights that though insight may be drawn, valuable information may also be lost through combined analysis and averaging. This underscores the importance of assaying scaffolds independently using individual peptides rather than mixture-based peptide libraries (including position-scanning libraries).[23] Our strategy accordingly enables accurate and informed selections of molecules with desired activities from within a combinatorial library (vide infra).

1. Cluster Analysis of MMPs. To compare primary sequence information of the MMPs with the specificity results obtained through inhibitor profiling, we hierarchically clustered MMPs across both these dimensions. Protein sequences were retrieved for 17 MMPs (including the 7 selected for this study) and clustered with ClustalW (Figure 3A). The cladogram obtained confirmed traditional classifications of MMPs based on sequence homology. MMPs -2 and -9, both gelatinases, were grouped closely together. Stromelysins, MMP-3 and MMP-10, were also clustered in the same clade, as were the membrane-type metalloproteases, MMPs -14 and -15. The MMPs were then clustered according to the inhibitor fingerprints obtained against the 1400 inhibitors. This produced a tree diagram as displayed in Figure 3B, representing classification on the basis of functional inhibition of the MMP panel. This analysis revealed that MMP-2 was the most distinct in its inhibition profile. MMPs -9 and -13 formed a sister pair, as did MMPs -8 and -14, highlighting the similarity in inhibitor preference among these enzymes and across traditional family clusters. Clustering was also performed for averaged potency data from the P_1' position (Figure 4). This provided a relatively unchanged cladogram. MMP-2 was again delineated from the other MMPs. MMPs -8 and -14 and MMPs -9 and -13 were further grouped as sister pairs, suggesting that contributions across P_1' positions were of predominant importance in overall clustering.

This inhibitor-based classification provides a useful way of looking at MMPs with functional relevance when attempting to design specific inhibitors against specific members of the family. This initial model provides preliminary relationships by incorporating inhibition-dependent profiles for MMP classification. This classification is distinct, indicating that inhibition selectivity and associations may not be sufficiently predicted from known substrates or primary sequence data alone. Similar conclusions have also been drawn through profiling cysteine proteases using PS peptide substrate libraries.[24]

The averaged P_1' data was also clustered across the 11 residues (Figure 4). This clearly discriminated the more potent residues ($\mathbf{C_p}$, **L**, **$_l$F**, and $\mathbf{S_f}$) from the other P_1' side chains. The generally weaker side chains (**I**, **V**, **K**, **D**, and **$_l$S**) were grouped closely together, with the mixed inhibitors ($\mathbf{C_h}$ and **F**) showing a closer relationship to one another relative to the other groups. This is consistent with the earlier analysis relating contributions of these P_1' side chains to overall potency.

Top 100 Analysis. We picked the best 100 inhibitors against each MMP and used Venn diagrams to evaluate the distributions of these hits across the seven MMP panel (Figure 5). These

(21) Whittaker, M.; Floyd, C. D.; Brown, P.; Gearing, A. J. H. *Chem. Rev.* **1999**, *99*, 2735−2776.
(22) Devel, L.; Rogakos, V.; David, A.; Makaritis, A.; Beau, F.; Cuniasse, P.; Yiotakis, A.; Dive, V. *J. Biol. Chem.* **2006**, *281*, 11152−11160.
(23) *Combinatorial Peptide Library Protocols*; Cabilly, S., Ed.; Humana Press: NJ, 1998.
(24) Choe, Y.; Leonetti, F.; Greenbaum, D. C.; Lecaille, F.; Bogyo, M.; Bromme, D.; Ellman, J. A.; Craik, C. S. *J. Biol. Chem.* **2006**, *281*, 12824−12832.

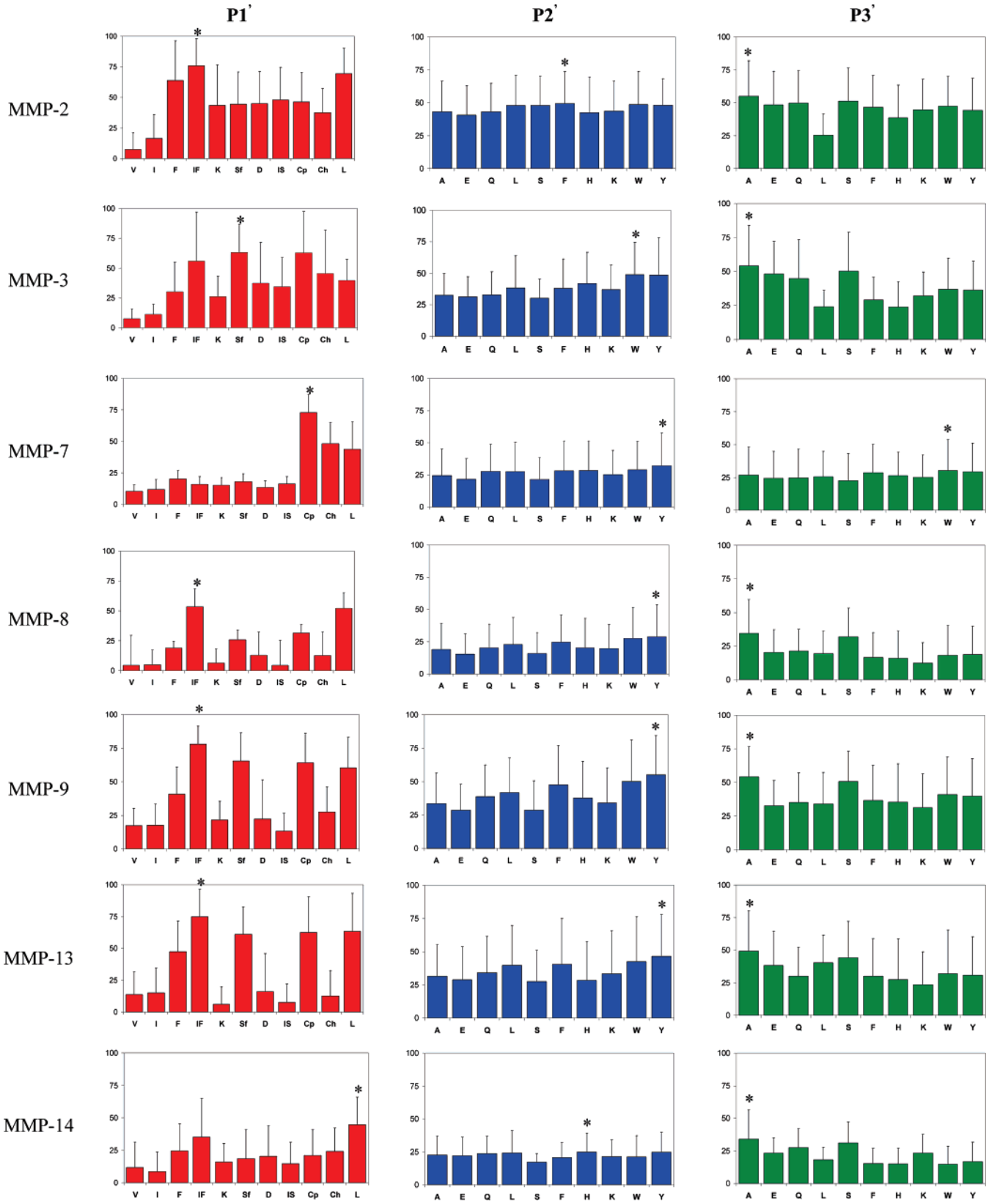

Figure 2. Averaged inhibition contributions across permuted P_1', P_2', and P_3' positions. Each bar represents averaged inhibition across inhibitors in the library presenting the relevant residue. The error bar denotes the standard deviation across each group of inhibitors. The asterisk (∗) highlights the residue contributing to the highest inhibition average in each graph.

represented inhibitors that displayed relative inhibition potencies of at least 75% against respective MMPs. Despite a considerable overlap in the inhibitors appearing in multiple top 100 lists (there were 375 unique scaffolds from the 700 total selected), we were able to identify individual inhibitors with varying degrees of selectivity against the MMPs. This included a total of 198 inhibitors (approximately 47.5% of the unique inhibitors scaffolds) that were selective against specific MMPs. The identities

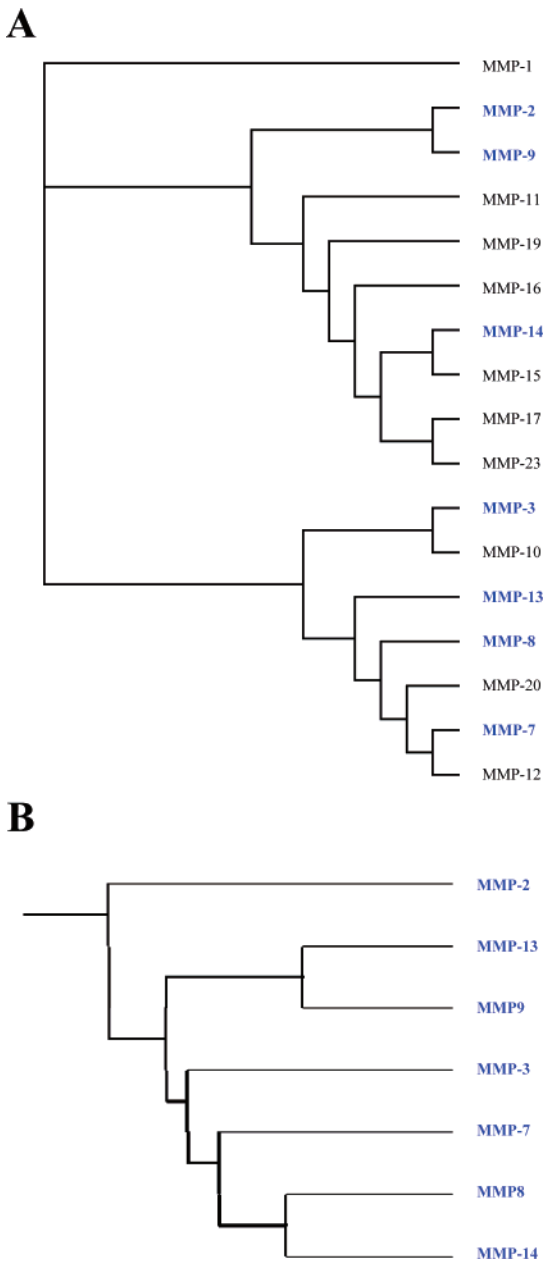

Figure 3. Cladograms of MMPs based on (A) sequence homology and (B) inhibitor fingerprints. Sequence data for each MMP was obtained from MEROPS, and the image was produced using the ClustalW software. Approximately 170aa for the active site of each protein were aligned and visualized by TreeView (http://taxonomy.zoology.gla.ac.uk/rod/treeview.html). MMPs used in this study are shown in blue and bold. For panel B, the seven-member MMP panel was clustered according to the complete inhibitor fingerprints obtained. Average linkage clustering was performed.

and specificities of these inhibitors are listed in Supporting Information Table S3A. We also uncovered inhibitors from this subset that exhibited potency against more than one MMP. Although no single inhibitor was potent against all 7 MMPs, a total of 13 were found to be potent against combinations of 5 MMPs (Supporting Information Table S3B). Ten of these inhibitors presented **L** in the P_1' position, confirming earlier analysis of this side chain as potent in broad-range MMP inhibitors. We also found that a total of 86, 47, and 31 inhibitors from the top 100 set that targeted combinations of two, three, and four MMPs, respectively (Figure 5B).

IC_{50} Measurements of Selected Inhibitors. For a more quantitative determination of the inhibition potencies, we subjected 11 inhibitors with differing specificity profiles to complete IC_{50} evaluation with the MMP panel (Table 1 and Supporting Information Figure S3). We selected inhibitors on the basis of broad-range as well as narrow-range potencies, as well as from results determined from the top 100 classification. We also attempted to characterize several inhibitors that appeared to discriminate only a single target or antitarget MMP. We predominantly selected representatives from P_1' $\mathbf{C_p}$ and **L** sublibraries for a more focused analysis on a subset of the whole data set, which is by no means exhaustive. Notwithstanding, we were able to confirm with IC_{50} measurements the predicted selectivity patterns for most of the inhibitors screened. The analysis shows that certain inhibitors were found to give high potencies across a wide range of MMPs. This included inhibitors like **5. C_p-W-A** and **6. C_p-Y-L** that provided low-nanomolar potencies against most of the MMPs screened. **6.** was also found to be one of the most potent inhibitors evaluated against the MMP-7 target, providing a strong IC_{50} value of 52 nM. Various other potent inhibitors were also uncovered against other MMPs. For example, **7. L-I-G** was found to be highly potent against MMPs -8, -9, and -13 with IC_{50} values of 8.8, 11, and 7.2 nM, respectively.

Narrow-range inhibitors uncovered included members from the $\mathbf{C_p}$ sublibraries presenting with **A** in the P_2' position that conferred 2−3-fold greater selectivity toward MMP-7 (a target MMP) over the other MMPs screened. Specifically **2. C_p-A-L**, **3. C_p-A-Y**, and **4. C_p-A-F** all gave low-nanomolar inhibition potency, 116, 168, and 172 nM, respectively. Another inhibitor, **1. F-E-A**, was also selective toward MMP-13 (an antitarget MMP) at an IC_{50} of 164 nM. GM6001 was also screened alongside the selected inhibitors and provided IC_{50} values consistent with those previously reported with these enzymes.[25] As expected, selected inhibitors presenting **V** and **I** at the P_1' position exhibited relatively weak IC_{50} values that were too low (>2 μM) to be determined accurately from the assay setup. We further observed that, apart from a few exceptions (7 out of 77 inhibition potencies, as underlined in Table 1), there was very good correlation with the relative potencies in the high-throughput screening and the IC_{50} values determined.

Docked Positions of Selected Inhibitors. Selected inhibitors were also employed for docking analysis with two representative MMPs. MMP-7, a short P_1' pocket enzyme, and MMP-2, a long P_1' pocket, were used to highlight the binding mode of the inhibitors (i.e., a broad-range inhibitor **C_p-Y-L** and a narrow-range inhibitor **C_p-A-F**) to the active sites of the enzyme in Figure 6 and Supporting Information Figure S4. As would be expected, the optimized docking configuration of the inhibitor/enzyme complexes revealed the inhibitors adopted an extended conformation, comfortably fitting along the substrate binding groove in the enzyme active site (Figure 6). The hydroxamate group from the inhibitor was observed to chelate to the bound zinc atom, while the $\mathbf{P_1'}$ side chains fitted nicely into the S_1' pockets. The potential docking configurations of potent MMP-7 inhibitors **C_p-A-F** and **C_p-Y-L** are displayed, indicating that both fitted nicely into the active sites of the MMP-7 (Figure 6, parts

(25) Grobelny, D.; Poncz, L.; Galardy, R. E. *Biochemistry* **1992**, *31*, 7152−7154.

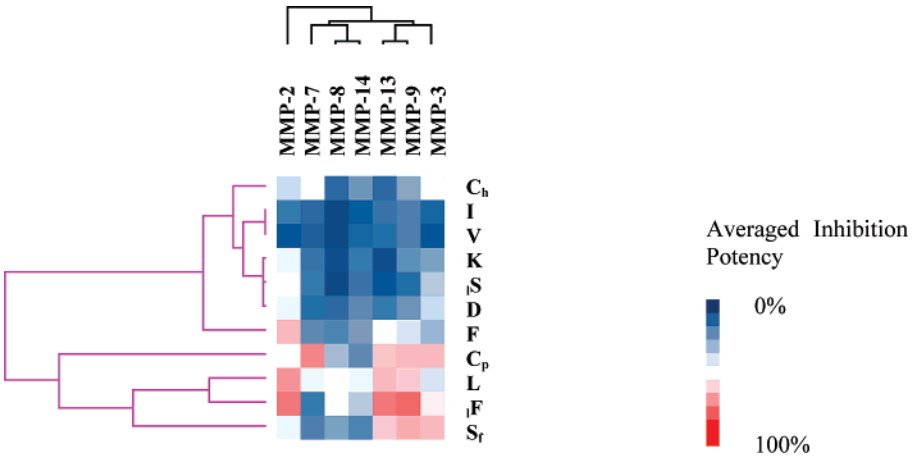

Figure 4. Hierarchical clustering across the P_1' position. The image was generated using Cluster and is presented in tree view (http://rana.lbl.gov/EisenSoftware.htm). Average linkage clustering was performed both across the MMP panel (tree in black) as well as across the P_1' substituents (tree in pink).

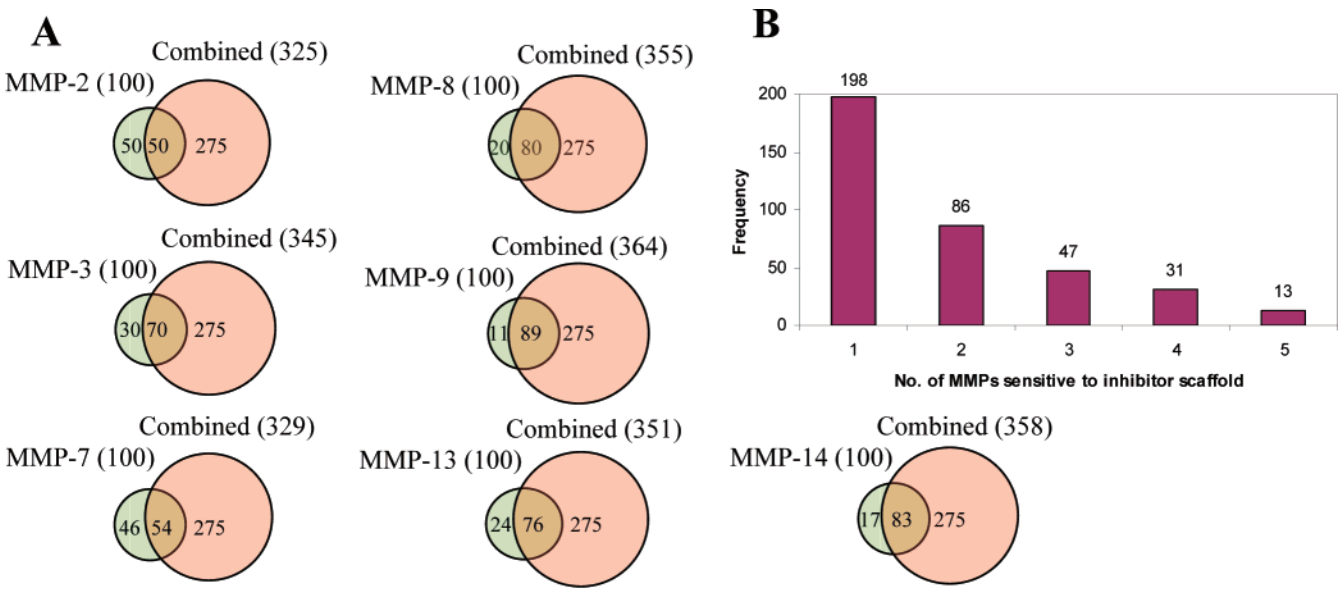

Figure 5. Distribution of the top 100 inhibitors. (A) Venn diagrams illustrations of the top 100 inhibitors against each MMP. (B) A total of 198 inhibitors out of the 375 unique scaffolds in the top 100 set were selective against individual MMPs. Thirteen broadly selective inhibitors were uncovered that appeared in the top 100 in at least five MMPs.

A and B). Docking of **C_p-A-F** with MMP-2 was unsuccessful (data not shown), potentially because of low binding affinity as indicated from the IC_{50} analysis (Table 1). The docking result for MMP-2 with **C_p-Y-L**, as shown in Figure 6C, indicates smaller side chains at the P_1' (such as **C_p**) bind well to the unobstructed and deep S_1' pocket of MMP-2. In addition, longer P_1' side chains (i.e., **L**) also docked successfully (Supporting Information Figure S4), thus accounting for the relatively high potency of these two side chains. It was further observed that the P_2' and P_3' positions of the inhibitor bound to solvent-accessible regions of the protein, partially accounting for the lower degree of selectivity observed from these sites. They could, however, contribute to overall inhibition potency through the formation of hydrogen bonds or other favorable electrostatic interactions with the protein.

Discussion

It has been a long-standing goal to develop inhibitors against MMPs as they have been implicated in many human diseases.[26] Various global formats have been introduced in attempts to provide a clear mechanistic and functional understanding of MMPs.[10,27−39] They include degenerated peptide libraries for

(26) Baker, A. H.; Edwards, D. R.; Murphy, G. *J. Cell. Sci.* **2002**, *115*, 3719−3727.
(27) Turk, B. E.; Huang, L. L.; Piro, E. T.; Cantley, L. C. *Nat. Biotechnol.* **2001**, *19*, 661−667.
(28) Sieber, S. A.; Niessen, S.; Hoover, H. S.; Cravatt, B. J. *Nat. Chem. Biol.* **2006**, *2*, 274−281.
(29) Chan, E. W. S.; Chattopadhaya, S.; Panicker, R. C.; Huang, X.; Yao, S. Q. *J. Am. Chem. Soc.* **2004**, *126*, 14435−14446.
(30) Lukacova, V.; Zhang, Y.; Mackov, M.; Baricic, P.; Raha, S.; Calvo, J. A.; Balaz, S. *J. Biol. Chem.* **2004**, *279*, 14194−14200.
(31) Sang, A. Q.; Douglas, D. A. *J. Protein Chem.* **1996**, *15*, 137−159.
(32) Levy, D. E.; Lapierre, F.; Liang, W.; Ye, W.; Lange, C. W.; Li, X.; Grobelny, D.; Casabonne, M.; Tyrell, D.; Holme, K.; Nadzan, A.; Galardy, R. E. *J. Med. Chem.* **1998**, *41*, 199−223.
(33) Smith, M. M.; Shi, L.; Navre, M. *J. Biol. Chem.* **1995**, *270*, 6440−6449.
(34) Deng, S.-J.; Bickett, D. M.; Mitchell, J. L.; Lambert, M. H.; Blackburn, R. K.; Carter, H. L., III; Neugebauer, J.; Pahel, G.; Weiner, M. P.; Moss, M. L. *J. Biol. Chem.* **2000**, *275*, 31422−31427.
(35) Netzel-Arnett, S.; Sang, Q.-X.; Moore, W. G. I.; Navre, M.; Birkedal-Hansen, H.; Van Wart, H. E. *Biochemistry* **1993**, *32*, 6427−6432.
(36) Teahan, J.; Harrison, R.; Izquierdo, M.; Stein, R. L. *Biochemistry* **1989**, *28*, 8497−8501.

Table 1. IC_{50} of Selected Inhibitors against Panel of Enzymes[a]

	Enzyme Inhibitor P_1'-P_2'-P_3'	MMP-2 IC_{50}/nM *(%inh)*	MMP-3 IC_{50}/nM *(%inh)*	MMP-7 IC_{50}/nM *(%inh)*	MMP-8 IC_{50}/nM *(%inh)*	MMP-9 IC_{50}/nM *(%inh)*	MMP-13 IC_{50}/nM *(%inh)*	MMP-14 IC_{50}/nM *(%inh)*
Selective Inhibitors	1. F-E-A	**>2000** *(2.2)*	**>2000** *(0)*	**>2000** *(17.9)*	**>2000** *(19.7)*	**>2000** *(33.1)*	**164****±n.d. *(91.7)*	**>2000** *(6.0)*
	2. C_p-A-L	**>2000** *(17.8)*	**>2000** *(23.6)*	**116**** ± 29 *(84.0)*	**963** ± 316 *(39.1)*	**383** ± 72 *(51.3)*	**687** ± 405 *(50.6)*	**>2000** *(11.0)*
	3. C_p-A-Y	**>2000** *(23.9)*	**>2000** *(43.6)*	**168****±111 *(79.0)*	**1650** ± 508 *(9.2)*	**379** ± 97 *(46.0)*	**1030** ± 430 *(46.3)*	**>2000** *(5.4)*
	4. C_p-A-F	**>2000** *(34.0)*	**>2000** *(27.6)*	**172**** ± 68 *(81.1)*	**1100** ± 343 *(16.7)*	**330** ± 44.8 *(51.9)*	**996** ± 520 *(46.1)*	**>2000** *(4.3)*
Potent, Broad Range Inhibitors	5. C_p-W-A	**203** ± 62 *(82.2)*	**299** ± 40 *(100)*	**173** ± 39 *(83.0)*	**34** ± 11 *(64.8)*	**11** ± 4.6 *(99.2)*	**33** ± 12 *(93.8)*	**199** ± 36 *(67.4)*
	6. C_p-Y-L	**472** ± 222 *(55.0)*	**165** ± 29 *(100)*	**52** ± 25 *(92.7)*	**209** ± 153 *(46.3)*	**39** ± 16 *(82.5)*	**12.4** ± 8.6 *(100)*	**223** ± 45 *(29.5)*
	7. L-I-G	**167** ± 125 *(81.0)*	**501**± 65 *(80.1)*	**138** ± 121 *(77.2)*	**8.8** ± 4.9 *(99.5)*	**11** ± 3.8 *(94.9)*	**7.2** ± 3.3 *(84.1)*	**81** ± 12 *(83.2)*
	8. L-V-L	**>2000** *(0)*	**569** ± 85 *(14.2)*	**98** ± 35 *(67.8)*	**451** ± n.d. *(16.5)*	**574** ± 90 *(30.1)*	**62** ± 41 *(4.9)*	**281** ± 150 *(23.0)*
	9. L-V-M	**1900** ± 980 *(0)*	**286** ± 81 *(25.1)*	**98** ± 35 *(69.2)*	**275** ± 235 *(8.3)*	**223** ± 50 *(35.9)*	**463** ± n.d. *(6.2)*	**133** ± 17 *(16.2)*
Non-Potent	10. I-L-L	**>2000** *(0)*	**>2000** *(15.8)*	**>2000** *(11.5)*	**>2000** *(0)*	**>2000** *(26.4)*	**>2000** *(68.4)*	**>2000** *(4.7)*
	11. V-L-L	**>2000** *(0)*	**>2000** *(12.7)*	**>2000** *(8.5)*	**>2000** *(0)*	**>2000** *(13.0)*	**>2000** *(75.8)*	**>2000** *(4.5)*
	12. GM6001	**17** ± 4 *(>90)*	**27** ± 4 *(>90)*	**41** ± 14 *(>90)*	**1.4** ± n.d. *(>90)*	**4.1** ± 1.0 *(>90)*	**3.2** ± 2.3 *(>90)*	**33** ± 1.3 *(>90)*

[a] Eleven inhibitors identified from the library were subjected to IC_{50} analysis for more detailed evaluation against all seven MMPs. The IC_{50} values obtained using a dilution series of each inhibitor are tabulated (shown in bold with error margins) together with the inhibition potencies obtained from the high-throughput screening (shown in italics). The molecules are grouped as follows: selective inhibitors in green, potent broad-range inhibitors in red, and nonpotent inhibitors in blue; a commercial broad-spectrum MMP inhibitor, GM6001, is shown in pink. Instances where the inhibition potencies were not predictive of the IC_{50} values obtained are underlined. (n.d., not determined).

the identification of potential MMP substrates,[27] the development of activity-based fluorescent probes to target these enzymes in vivo,[28,29] the use of various computational methods for the discovery of enzyme inhibitors.[10,30,31] and structure−activity studies for inhibitor design.[32] Other efforts to probe MMP substrate specificity through phage display,[33,34] synthetic peptide substrates,[35,36] and mixture-based libraries,[37,38] however, did not always provide accurate models when compared with native substrates,[39] limiting the immediate utility of such approaches toward inhibitor design and development (Supporting Information Table S4).

We herein present, to our knowledge, the first large-scale inhibitor library to comprehensively and systematically address variations in inhibitor selectivity across metalloproteases. By adopting a high-throughput screening format and a focused library of inhibitors, we were able to readily obtain unique inhibitor fingerprints against a panel of seven representative MMPs. Further analysis of the inhibition patterns revealed unique clusters that were unlike traditional MMP groupings. This new classification on the basis of inhibitor selectivity has significance toward future design of targeted inhibitors against specific MMPs. Moreover, it was established that MMPs from different families could exhibit very similar inhibitor fingerprints, indicating that they could potentially be targeted with very closely related inhibitors. This was so in the case of MMPs -8 and -14 as well as MMPs -9 and -13. Computational methods have also revealed similar homologies across MMP active sites. Lukacova et al. have examined a range of MMPs active sites using force field interactions, which revealed similarities between MMPs -3 and -7 as well as among MMPs -2, -3, -8, and -12 and MMPs -3, -7, -8, and -12.[30] This correlates well with our own findings with MMPs -3 and -7 clustering closely to one another (Figure 3). Consistent with what has been established across MMPs, we found that the S_1' pocket was the most crucial position in determining inhibitor preference. The P_2' and P_3' positions were nevertheless important in conferring inhibitor selectivity across various MMPs.[40,41]

One clear benefit of our strategy is the design of a combinatorial library with discrete sequences. For synthetic convenience, PS libraries have traditionally been applied for high-throughput studies in examining global preference toward effectors or inhibitors.[42] This method assumes that contributions across different positions of the library do not significantly contribute to potency. Though we were able to overcome the synthetic challenge in creating a whole library of uniquely defined inhibitors, we simplified our data analysis in the same

(37) Berman, J.; Green, M.; Sugg, E.; Anderegg, R.; Millington, D. S.; Norwood, D. L.; McGeehan, J.; Wiseman, J. *J. Biol. Chem.* **1992**, *267*, 1434−1437.
(38) McGeehan, G. M.; Bickett, D. M.; Green, M.; Kassel, D.; Wiseman, J. S.; Berman, J. *J. Biol. Chem.* **1994**, *269*, 32814−32820.
(39) Nagase, H.; Fields, G. B. *Biopolymers* **1996**, *40*, 399−416.
(40) Kontogiorgis, C. A.; Papaioannou, P.; Hadjipavlou-Litina, D. J. *Curr. Med. Chem.* **2005**, *12*, 339−355.
(41) Verma, R. P.; Hansch, C. *Bioorg. Med. Chem.* **2007**, *15*, 2223−2268.
(42) Pinilla, C.; Appel, J. R.; Borras, E.; Houghten, R. A. *Nat. Med.* **2003**, *9*, 118−122.

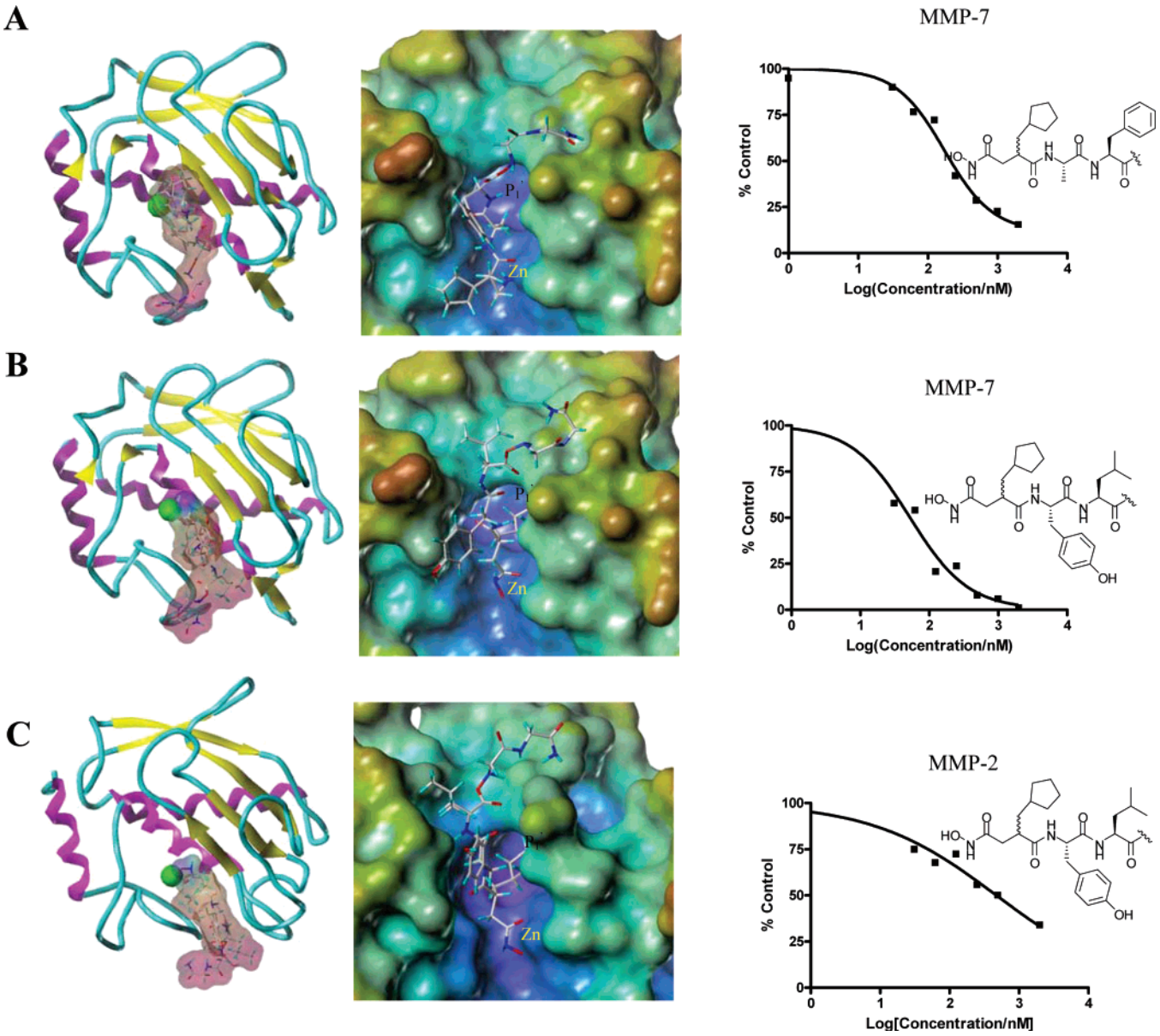

Figure 6. Docking configurations of selected inhibitors with MMPs. Both a potent, selective (**C_p-A-F**) and potent broad-spectrum inhibitor (**C_p-Y-L**) are used to display potential binding configurations in the enzyme active site of MMP-7 (short S_1' binding site) and MMP-2 (deep S_1' binding site). (A) MMP-7 complexed with **C_p-A-F** and (B) **C_p-Y-L**. The IC_{50} profiles with these inhibitors are shown (inset). (C) MMP-2 complexed with **C_p-Y-L**. The IC_{50} profile with this inhibitor is shown (inset). The zinc ion in the active site is shown as a green sphere.

way that synthesis is simplified in PS libraries, by averaging effects from alternative positions. Interestingly, consolidating our data in this manner led to a significant loss of information, especially in deciphering selective inhibitors for a group of highly similar and conserved enzymes (Figure 3 could very well represent results from a PS library designed for the same purpose), underscoring the limitation of PS libraries in the accurate determination of closely related inhibitors.

Our detailed analysis enabled us to identify inhibitors that were both potent and selective against various MMPs. It is important to establish selectivity at the early screening stage especially in providing a clear understanding of undesirable off-target effects of these inhibitors. This could be factored in during lead optimization so as to maximize success in drug development, especially among a highly similar group of proteins like the MMPs.

Our data set has provided a range of inhibitors which demonstrated potency against certain specific MMPs as well as potency across members of one or more MMP families. In particular, further analysis has led to the discovery of certain scaffolds that also exhibit good potency with several MMPs and may be developed and optimized for greater selectivity in the design of selective and potent MMP inhibitors for therapeutic applications. Significantly we identified potent chemical scaffolds, specifically within the **C_p** and **L** sublibraries, that could selectively inhibit MMP-7, a known target in pancreatic cancer and intestinal adenoma.[5] Some of these inhibitors displayed modest selectivities of 2−3-fold against MMP-7 relative to all other MMPs in the panel, and high selectivities of more than 10-fold against certain MMPs, thereby displaying promise for further therapeutic development. We also identified several broad-spectrum inhibitors with low-nanomolar potency against

a variety of MMPs. Notably, we have so far only explored a subset of the complete screening results in detail, and there are potentially many other inhibitors characterized within our data set with desirably tuned selectivity.

Conclusion

In conclusion, we have presented a strategy for the potential discovery of selective and potent MMP inhibitors. We find that, with a modest library size of 1400 inhibitors, we were able to functionally discriminate this highly homologous group of enzymes through the use of novel fingerprinting experiments with inhibitors that address not only their potency but, more importantly, their selectivity. This potentially provides a good therapeutic resource in the treatment of cancers and other disorders, as well as in further structure−activity assessments for improved drug design and discovery against MMPs.

Supporting Information Available: Lists of MMPs, library design for 1400-member hydroxamate peptides, selective and broad-range inhibitors uncovered, motif selectivity comparisons. Figures of inhibition potencies, reagents and conditions, IC_{50} determination, and docking configurations of selected inhibitors with MMPs. This material is available free of charge via the Internet at http://pubs.acs.org.

JA070870H